Electronic Supplementary Material (ESI) for Journal of Materials Chemistry A.

Supplementary information

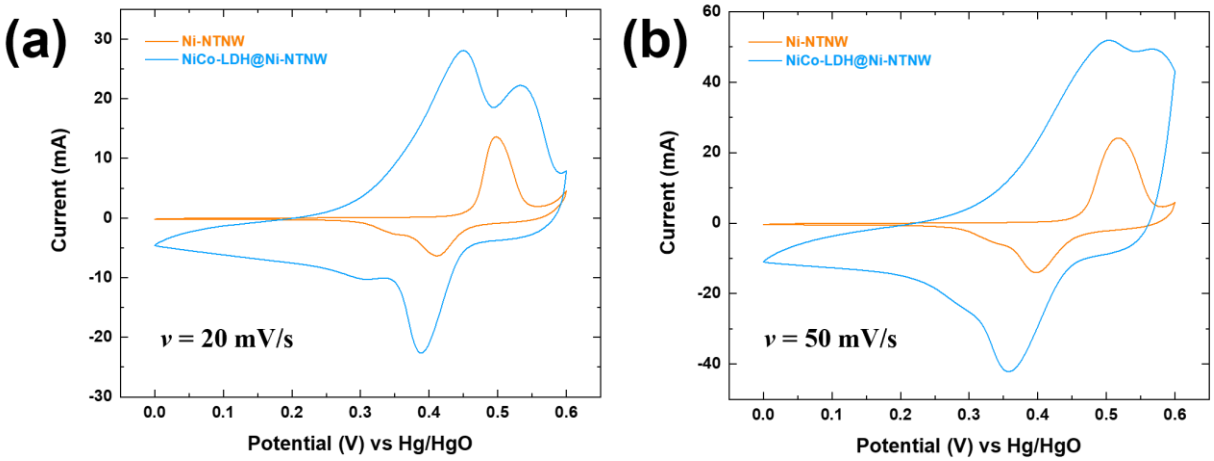

Fig. S1 CV of Ni-NTNW and NiCo-LDH@Ni-NTNW electrodes at scan rates of (a) 20 mV/s and (b) 50 mV/s.

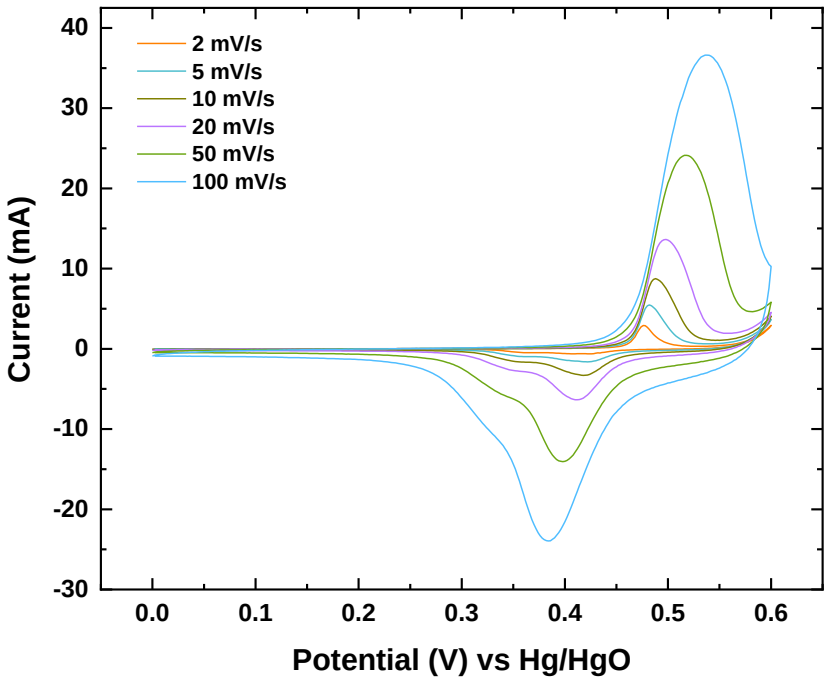

Fig. S2 CV curves of Ni-NTNW at different scan rates between 2-100 mV/s.

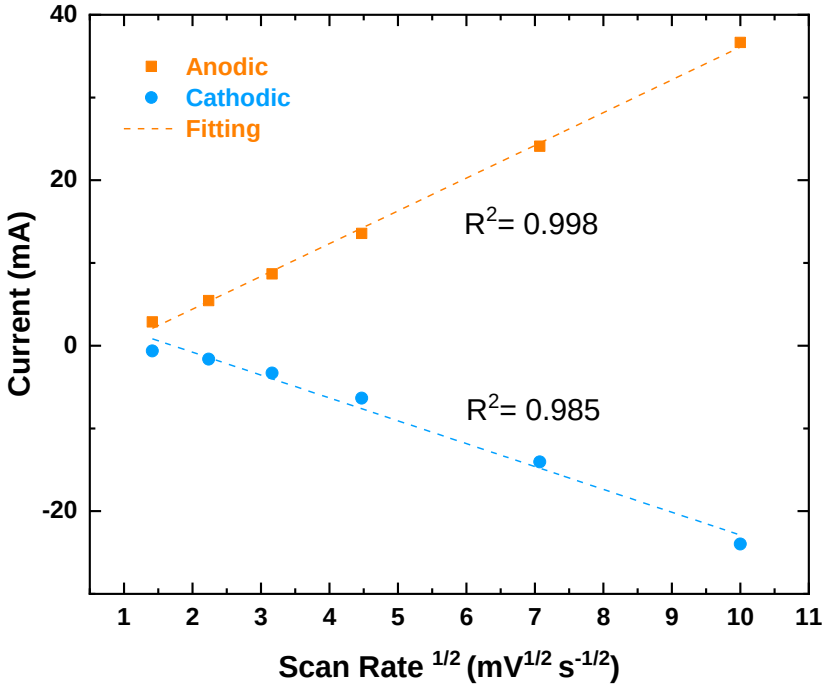

Fig. S3 The oxidation and reduction peak currents as a function of $v^{1/2}$ of Ni-NTNW electrode.

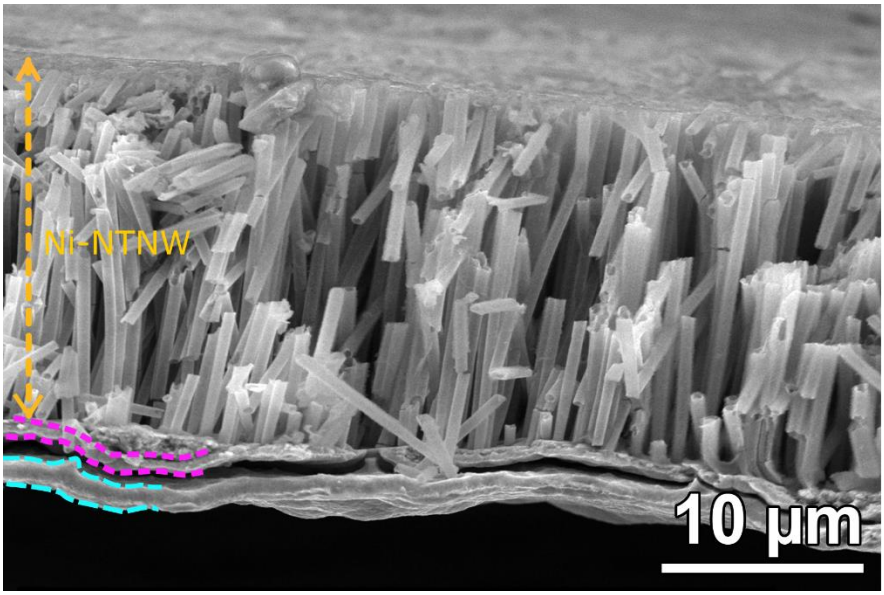

Fig. S4 SEM cross-sectional micrograph of the Ni-NTNW based electrode (with 400 nm nanotubes).

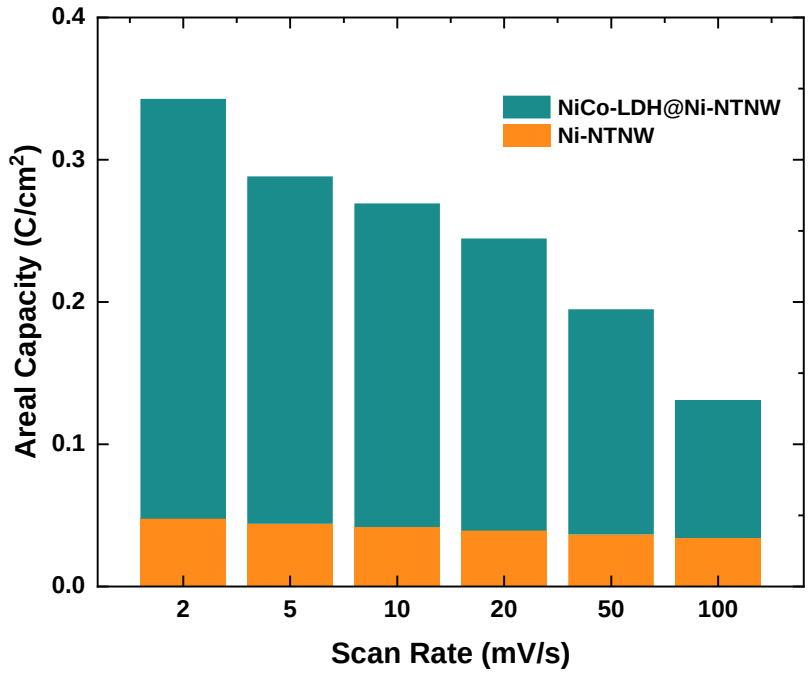

Fig. S5 Areal capacities of Ni-NTNW and NiCo-LDH@Ni-NTNW electrodes estimated from CV curves at different scan rates.

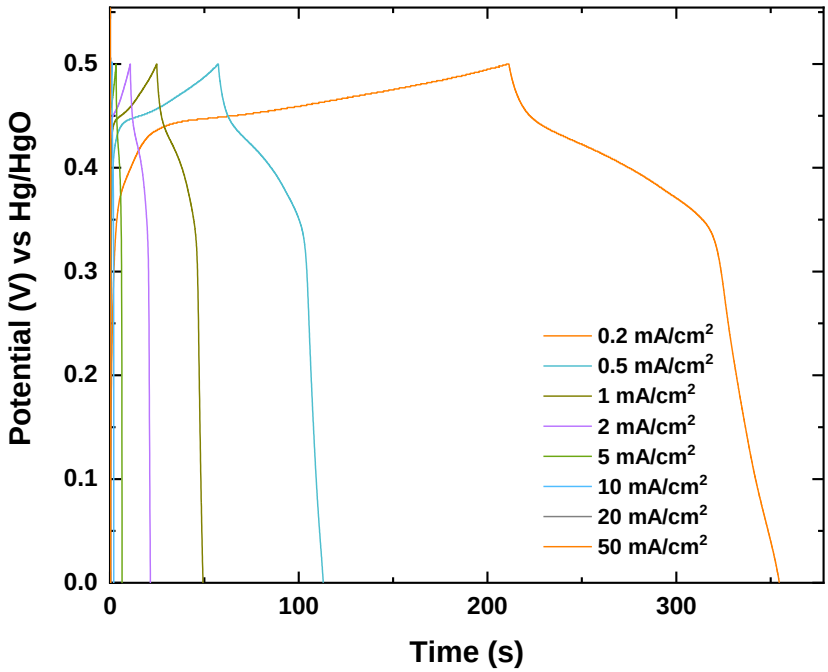

Fig. S6 GCD curves for Ni-NTNW electrode at different current densities between 0.2 and 50 mA/cm^2.

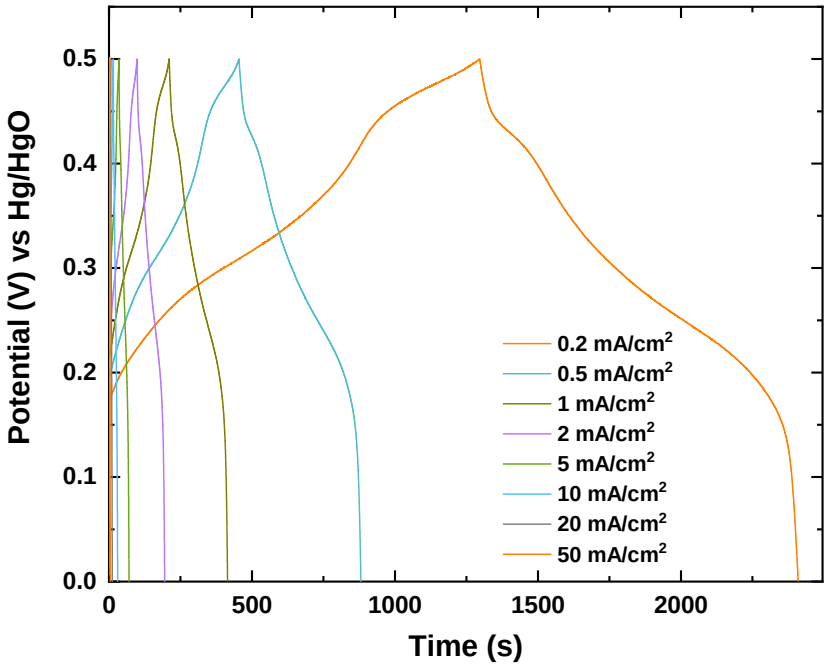

Fig. S7 GCD curves for NiCo-LDH@Ni-NTNW electrode at different current densities between 0.2 and 50 mA/cm2.

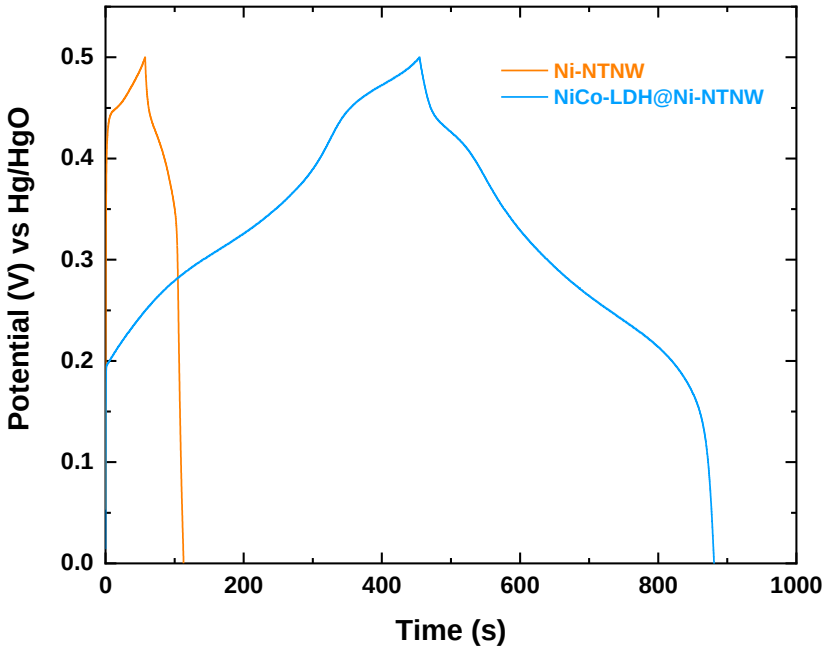

Fig. S8 GCD curves of Ni-NTNW and NiCo-LDH@Ni-NTNW electrodes at 0.5 mA/cm^2.

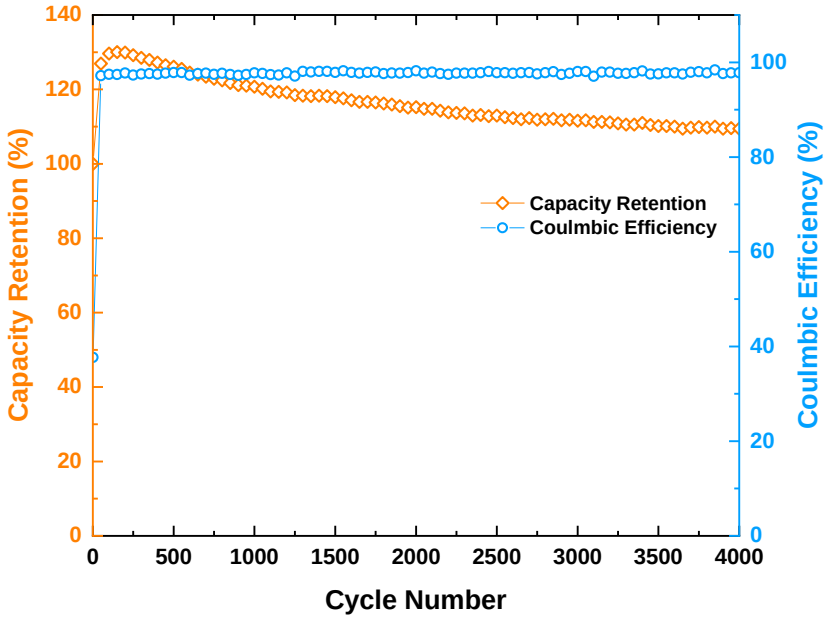

Fig. S9 Cycling stability of the Ni-NTNW electrode at current density of 10 mA/cm^2.

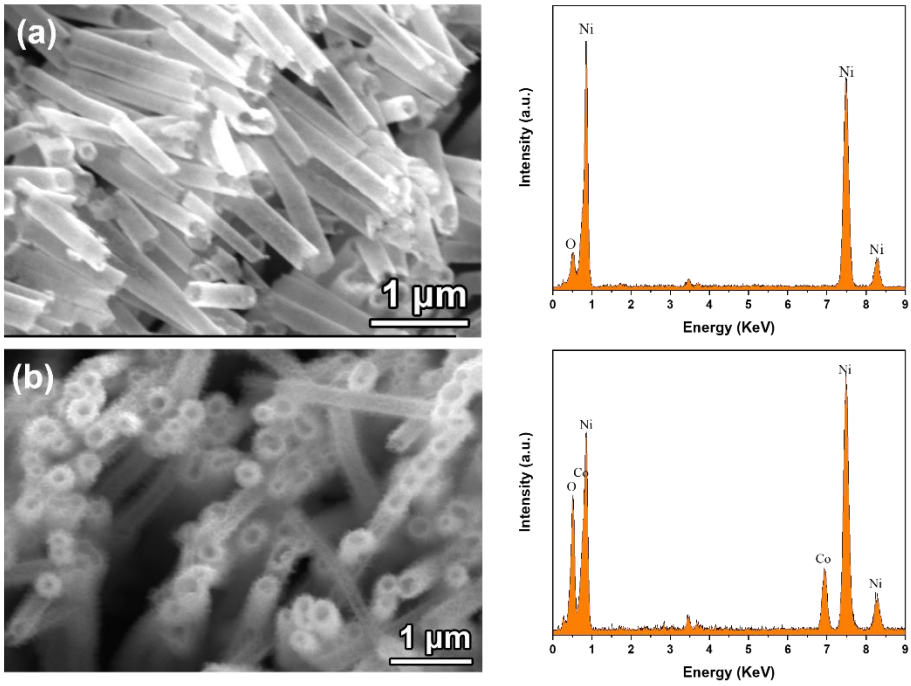

Fig. S10 SEM and EDX of (a) Ni-NTNW and (b) NiCo-LDH@Ni-NTNW electrodes after cycling test.

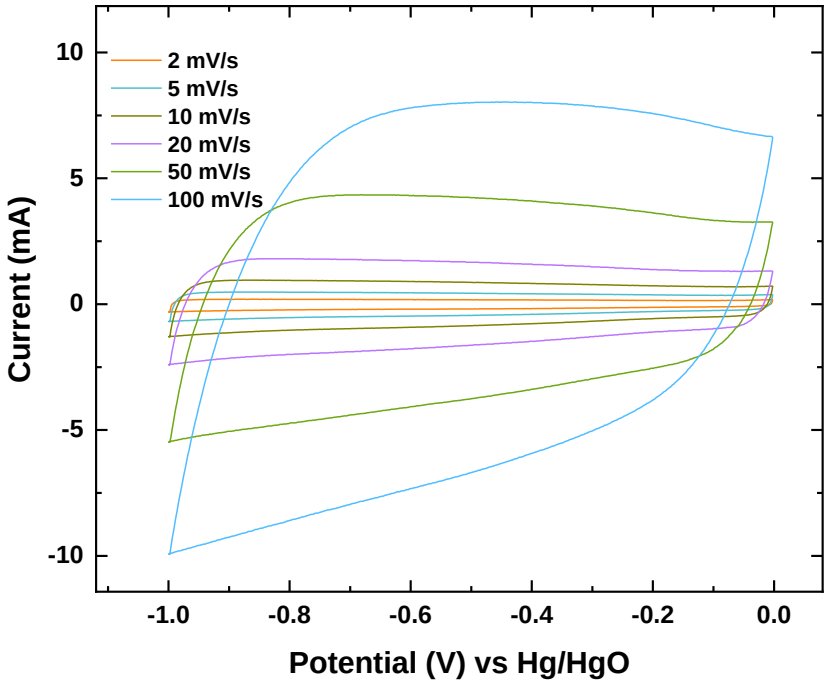

Fig. S11 CV curves of AC electrode at different scan rates between 2-100 mV/s.

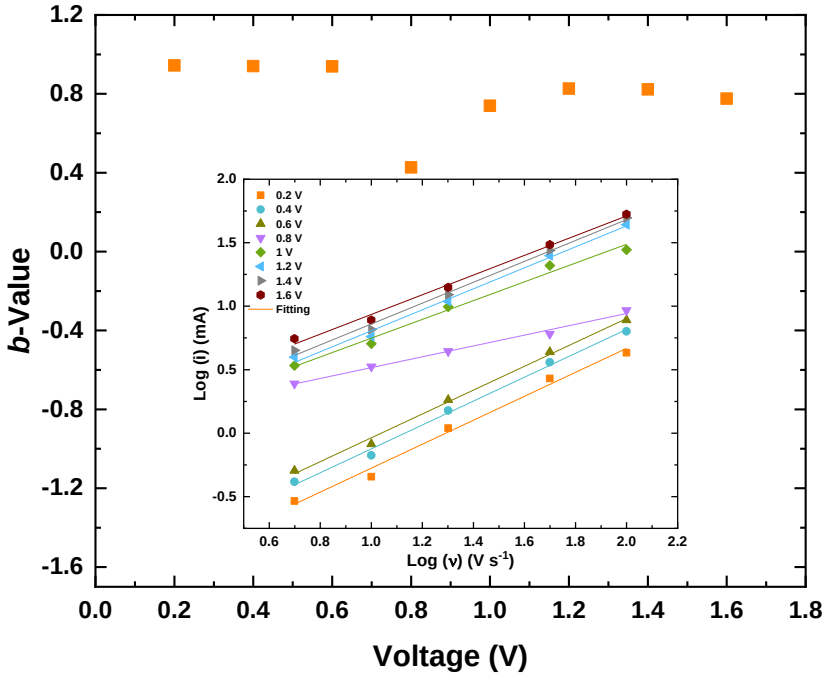

Fig. S12 *b*-Values for the assembled HSC at different voltages (Inset: the plots of log *I* as a function of log *v* at different stages of the CV potential window).

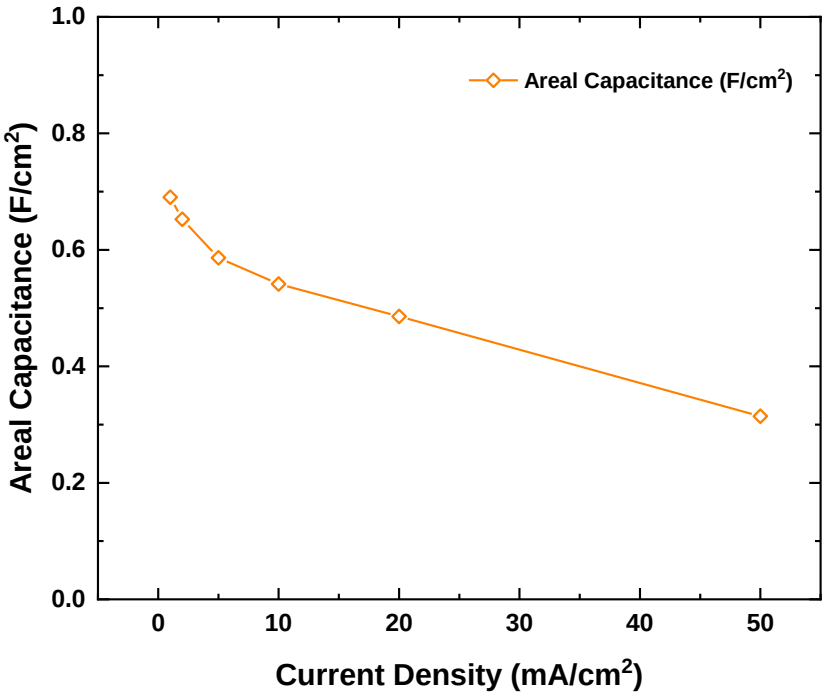

Fig. 13 Areal capacitance the HSC device at different current densities.

Table S1. Performance comparison of NiCo-LDH@Ni-NTNW electrode with recently reported NiCo-based battery-type electrodes in three-electrode setup.

Electroactive material	Current collector	Current density	Electrolyte	Capacity	Ref.
$NiCoP/Ti_3C_2$ MXene	3D printed CNT based ink	-	2 M KOH	68.5 C/cm^3 10 C/cm^2	[1]
NiCo–LDH	Ni–coated textile	1 A/g	1 M KOH	420 C/g	[2]
$Ag@NiCo_2S_4$	WC	1 mA/cm^2	6 M KOH	341 C/g 3.04 C/cm^2	[3]
$Co(OH)_2$	CW	1 mA/cm^2	2 M KOH	261 C/g 1.48 C/cm^2	[4]
NiO/ZnO	Ni foam	1.3 A/g	3 M KOH	248.5 C/g	[5]
NiCo-LDH/Co_9S_8	Ni foam	4 A/g	1 M KOH	~742 C/g *	[6]
Co-doped $Ni_{11}(HPO_3)_8(OH)_6$	Ni foam	0.5 A/g	3 M KOH	300.6 C/g	[7]
$NiCo_2S_4$	Ni foam	2 A/g	6 M KOH	508 C/g	[8]
2D/2D NiCo-MOF@GO	-	0.5 A/g	2 M KOH	413.6 C/g	[9]
Honeycomb Co@$Co(OH)_2$ sheets	Cellulose paper	2 mA/cm^2	6 M KOH	479 C/g 0.321 C/cm^2	[10]
Ni-Co LDH nanorods	Carbon nanofiber	0.02 mA/cm^2	1 M NaOH	551.2 C/g 0.011 C/cm^2	[11]
mesoporous network-like $NiCo_2O_4$	Carbon cloth	0.33 mA/cm^2	3 M KOH	16.2 C/cm^3 0.29 C/cm^2	[12]
NiCo-LDH@Ni-NTNW electrode	Integrated Ni supporting layer	0.2 mA/cm^2	1 M KOH	126.4 C/cm^3 601.0 C/g 0.252 C/cm^2	This work

* Estimated from specific capacitance figure

WC: wood-derived carbon

CW: carbonized wood

NGP: Ni/graphite/paper

Table S2. Comparison of electrochemical performance of our NiCo-LDH@Ni-NTNW//AC hybrid supercapacitor with state-of-the-art symmetric/asymmetric and hybrid supercapacitors with high volumetric capacitance and energy density.

Positive electrode	Negative electrode	Current density (mA/cm^2)	Gravimetric capacitance (F/g)	Areal capacitance (F/cm^2)	Volumetric capacitance (F/cm^3)	Capacitance Retention/ Cycles	Voltage (V)	Energy Density (mWh/cm^3)	Ref.
Mesoporous network-like $NiCo_2O_4$	Mesoporous network-like $NiCo_2O_4$	0.33	269	0.09	5	89% 4000	1	0.69 *	[12]
$CuCo_2O_4$	AC	1	-	0.262 **	2.62 **	82% 3000	1.5	0.81	[13]
MnO_2/TCC	TCC	2	45.3	1.5	16.8	96% 20000	2	9.4	[14]
NiCoP/Ti_3C_2 MXene	AC	2	-	3.29	10.97	87.5% 5000	1.4	2.2	[1]
NiCo-LDH@Ni-coated textile	NiCo-LDH@Ni-coated textile	-	-	-	-	-	0.65	1.25	[2]
Co_9S_8	Co_3O_4@RuO_2	2.5	-	0.34	4.28	90.2% 2000	1.6	1.44	[15]
WC@Ag@ $NiCo_2S_4$	WC@Ag	1	40.2	1.87	11.3	87.7% 10000	1.5	3.93	[3]
$Co(OH)_2$@CW	CW	1	34.8	2.2	14.19	85% 10000	1.5	4.45	[4]

$Ni(OH)_2$	Mn_3O_4	1	-	-	2.07	83.3% 12000	1.3	0.35	[16]
$GF/NiCo_2S_4$	GF	0.5	-	0.568	39.4	92% 2000	1.5	12.3	[17]
NiCo-LDH@Ni-NTNW	AC	1	142.6	0.69	76.7	124% 20000	1.6	14.8	This work

* calculated based on the mass loading

** estimated from specific capacitance figure

TCC: porous carbon cloth

GF: graphene fiber

Table S3. Cyclic stability comparison of our NiCo-LDH@Ni-NTNW//AC hybrid supercapacitor with recently reported asymmetric and hybrid supercapacitors with high-capacitance retention.

Device composition	Current density	Cycles	Retention	Ref.
CNTs/NiCo LDH //AC	5 A/g	10000	99.4 %	[18]
PPNF@Co−Ni MOF//CNF-G	10 A/g	10000	100 %	[19]
Layered CuCo hydroxide//ACC	8.33 mA/cm^2	3500	96.55%	[20]
NiCoP/Ti_3C_2 MXene//AC	12 mA/cm^2	5000	87.5%	[1]
WC@Ag@$NiCo_2S_4$// WC@Ag	50 mA/cm^2	10000	87.7%	[3]
$Co(OH)_2$@CW//CW	50 mA/cm^2	10000	85%	[4]
$Ni(OH)_2$//Mn_3O_4	-	12000	83.3%	[16]
NiCo-LDH//CNT	4 A/g	5000	103.9 %	[21]
NiCo-LDH//graphene	-	700	110 %	[22]
NiCo-LDH@Ni-NTNW//AC	20 mA/cm^2	20000	124 %	This work

AC: activated carbon

ACC: activated carbon cloth

References

[1] L. Yu, W. Li, C. Wei, Q. Yang, Y. Shao, J. Sun, 3D Printing of NiCoP/Ti3C2 MXene Architectures for Energy Storage Devices with High Areal and Volumetric Energy Density, Nano-Micro Lett. 12 (2020) 1–13. https://doi.org/10.1007/s40820-020-00483-5.

[2] Y.M. Jeong, I. Son, S.H. Baek, Binder–free of NiCo–layered double hydroxides on Ni–coated textile for wearable and flexible supercapacitors, Appl. Surf. Sci. 467–468 (2019) 963–967. https://doi.org/10.1016/j.apsusc.2018.10.252.

[3] F. Wang, X. Liu, G. Duan, H. Yang, J.Y. Cheong, J. Lee, J. Ahn, Q. Zhang, S. He, J. Han,

Y. Zhao, I.D. Kim, S. Jiang, Wood-Derived, Conductivity and Hierarchical Pore Integrated Thick Electrode Enabling High Areal/Volumetric Energy Density for Hybrid Capacitors, Small. 17 (2021) 1–10. https://doi.org/10.1002/smll.202102532.

[4] Y. Wang, X. Lin, T. Liu, H. Chen, S. Chen, Z. Jiang, J. Liu, J. Huang, M. Liu, Wood-Derived Hierarchically Porous Electrodes for High-Performance All-Solid-State Supercapacitors, Adv. Funct. Mater. 28 (2018). https://doi.org/10.1002/ADFM.201806207.

[5] G.-C. Li, P.-F. Liu, R. Liu, M. Liu, K. Tao, S.-R. Zhu, M.-K. Wu, F.-Y. Yi, L. Han, MOF-derived hierarchical double-shelled NiO/ZnO hollow spheres for high-performance supercapacitors, Dalt. Trans. 45 (2016) 13311–13316. https://doi.org/10.1039/C6DT01791F.

[6] G. Yilmaz, K.M. Yam, C. Zhang, H.J. Fan, G.W. Ho, In Situ Transformation of MOFs into Layered Double Hydroxide Embedded Metal Sulfides for Improved Electrocatalytic and Supercapacitive Performance, Adv. Mater. 29 (2017). https://doi.org/10.1002/ADMA.201606814.

[7] B. Li, Y. Shi, K. Huang, M. Zhao, J. Qiu, H. Xue, H. Pang, Cobalt-Doped Nickel Phosphite for High Performance of Electrochemical Energy Storage, Small. 14 (2018). https://doi.org/10.1002/SMLL.201703811.

[8] B.Y. Guan, L. Yu, X. Wang, S. Song, X.W.D. Lou, Formation of Onion-Like NiCo2S4 Particles via Sequential Ion-Exchange for Hybrid Supercapacitors, Adv. Mater. 29 (2017). https://doi.org/10.1002/ADMA.201605051.

[9] S. Li, C. Shi, Y. Pan, Y. Wang, 2D/2D NiCo-MOFs/GO hybrid nanosheets for high-performance asymmetrical supercapacitor, Diam. Relat. Mater. 115 (2021) 108358. https://doi.org/10.1016/j.diamond.2021.108358.

[10] C. Wan, Y. Jiao, D. Liang, Y. Wu, J. Li, A Geologic Architecture System-Inspired Micro-/Nano-Heterostructure Design for High-Performance Energy Storage, Adv. Energy Mater. 8 (2018). https://doi.org/10.1002/AENM.201802388.

[11] F. Lai, Y. Huang, Y.E. Miao, T. Liu, Controllable preparation of multi-dimensional hybrid materials of nickel-cobalt layered double hydroxide nanorods/nanosheets on electrospun carbon nanofibers for high-performance supercapacitors, Electrochim. Acta. 174 (2015)

456–463. https://doi.org/10.1016/J.ELECTACTA.2015.06.031.

[12] S. Gao, F. Liao, S. Ma, L. Zhu, M. Shao, Network-like mesoporous NiCo2O4 grown on carbon cloth for high-performance pseudocapacitors, J. Mater. Chem. A. 3 (2015) 16520–16527. https://doi.org/10.1039/C5TA02876K.

[13] Q. Wang, D. Chen, D. Zhang, Electrospun porous CuCo2O4 nanowire network electrode for asymmetric supercapacitors, RSC Adv. 5 (2015) 96448–96454. https://doi.org/10.1039/C5RA21170K.

[14] H. Wang, C. Xu, Y. Chen, Y. Wang, MnO2 nanograsses on porous carbon cloth for flexible solid-state asymmetric supercapacitors with high energy density, Energy Storage Mater. 8 (2017) 127–133. https://doi.org/10.1016/J.ENSM.2017.05.007.

[15] J. Xu, Q. Wang, X. Wang, Q. Xiang, B. Liang, D. Chen, G. Shen, Flexible Asymmetric Supercapacitors Based upon Co9S8 Nanorod//Co3O4@RuO2 Nanosheet Arrays on Carbon Cloth, ACS Nano. 7 (2013) 5453–5462. https://doi.org/10.1021/NN401450S.

[16] J.-X. Feng, S.-H. Ye, X.-F. Lu, Y.-X. Tong, G.-R. Li, Asymmetric Paper Supercapacitor Based on Amorphous Porous Mn3O4 Negative Electrode and Ni(OH)2 Positive Electrode: A Novel and High-Performance Flexible Electrochemical Energy Storage Device, ACS Appl. Mater. Interfaces. 7 (2015) 11444–11451. https://doi.org/10.1021/ACSAMI.5B02157.

[17] W. Cai, T. Lai, J. Lai, H. Xie, L. Ouyang, J. Ye, C. Yu, Transition metal sulfides grown on graphene fibers for wearable asymmetric supercapacitors with high volumetric capacitance and high energy density, Sci. Reports 2016 61. 6 (2016) 1–9. https://doi.org/10.1038/srep26890.

[18] M. Huang, Y. Wang, J. Chen, D. He, J. He, Y. Wang, Biomimetic design of Ni Co LDH composites linked by carbon nanotubes with plant conduction tissues characteristic for hybrid supercapacitors, Electrochim. Acta. 381 (2021) 138289. https://doi.org/10.1016/J.ELECTACTA.2021.138289.

[19] D. Tian, N. Song, M. Zhong, X. Lu, C. Wang, Bimetallic MOF Nanosheets Decorated on Electrospun Nanofibers for High-Performance Asymmetric Supercapacitors, (2019). https://doi.org/10.1021/acsami.9b16420.

[20] A.D. Deshmukh, A.R. Urade, A.P. Nanwani, K.A. Deshmukh, D.R. Peshwe, P. Sivaraman, S.J. Dhoble, B.K. Gupta, Two-Dimensional Double Hydroxide Nanoarchitecture with High Areal and Volumetric Capacitance, ACS Omega. 3 (2018) 7204–7213. https://doi.org/10.1021/acsomega.8b00596.

[21] R. Ramachandran, Y. Lan, Z.X. Xu, F. Wang, Construction of NiCo-Layered Double Hydroxide Microspheres from Ni-MOFs for High-Performance Asymmetric Supercapacitors, ACS Appl. Energy Mater. 3 (2020) 6633–6643. https://doi.org/10.1021/acsaem.0c00790.

[22] X. Sun, G. Wang, H. Sun, F. Lu, M. Yu, J. Lian, Morphology controlled high performance supercapacitor behaviour of the Ni–Co binary hydroxide system, J. Power Sources. 238 (2013) 150–156. https://doi.org/10.1016/J.JPOWSOUR.2013.03.069.